Replica Density Functional Study of One-Dimensional Hard Core Fluids in Porous Media

Hendrik Reich[1] and Matthias Schmidt[2,3]

A binary quenched-annealed hard core mixture is considered in one dimension in order to model fluid adsorbates in narrow channels filled with a random matrix. Two different density functional approaches are employed to calculate adsorbate bulk properties and interface structure at matrix surfaces. The first approach uses Percus' functional for the annealed component and an explicit averaging over matrix configurations; this provides numerically exact results for the bulk partition coefficient and for inhomogeneous density profiles. The second approach is based on a quenched-annealed density functional whose results we find to approximate very well those of the former over the full range of possible densities. Furthermore we give a derivation of the underlying replica density functional theory.

KEY WORDS: Density functional theory; quenched-annealed fluid mixtures; hard core models in one dimension; random porous media.

1. INTRODUCTION

The one-dimensional hard rod model[1] continuous to be an invaluable test bed for theoretical work as it provides the possibility to compare approximations to exact results. Recent examples of this strategy include investigations of depletion interactions in binary mixtures where one of the components is viewed as an agent that mediates an effective

[1] Institut für Theoretische Physik II, Heinrich-Heine-Universität Düsseldorf, Universitätsstraße 1, D-40225 Düsseldorf, Germany.
[2] Soft Condensed Matter, Debye Institute, Utrecht University, Princetonplein 5, 3584 CC Utrecht, The Netherlands.
[3] On leave from: Institut für Theoretische Physik II, Heinrich-Heine-Universität Düsseldorf, Universitätsstraße 1, D-40225 Düsseldorf, Germany; e-mail: mschmidt@thphy.uni-duesseldorf.de

interaction between particles of the other component,[2,3] a model colloid-polymer mixture[4] where particles representing polymers can freely penetrate, dynamical density functional theory[5,6] concerned with time-dependent transport phenomena, as well as a model porous medium[7] of lines of random length accessible to the fluid particles. As concerns equilibrium statistical mechanics, Percus' exact free energy functional for pure systems[8] and (additive) mixtures of particles with different sizes,[9] provides a framework to compute thermodynamics, density distributions, and correlation functions in arbitrary inhomogeneous situations.

Fluids adsorbed in disordered matrices are often described in the context of so-called quenched-annealed (QA) fluid mixtures, where particles of the quenched component act as randomly distributed obstacles exerting an external potential on particles of the annealed component.[10,11] The matrix particles are distributed according to the Hamiltonian of the quenched component, and hence can be treated with liquid state theory. The crucial difference to an equilibrium system of two annealed components is that the distribution of matrix particles is unaffected by the presence of the annealed component. As one is interested in the typical behavior of the system, a double average over the annealed degrees of freedom and over the quenched disorder is required. A short overview of this theoretical framework is given below. One standard approach to tackle fluid structure and phase behavior of QA models is via the replica Ornstein-Zernike relations[10,11] supplemented with appropriate closure relations. Many standard liquid integral equation theories have been carried over to the QA case. The basic quantities in terms of which these theories are formulated are two-body (and possibly higher) correlation functions.

Recently it was proposed to rather work directly on the level of the free energy functional, pre-averaged over the disorder.[12] Correlation functions can be obtained subsequently, in particular the hierarchy of direct correlation functions is obtained through functional differentiation with respect to the density fields. The advantage of formulating the theory on the one-body level of the density fields is that inhomogeneous situations, e.g. at free interfaces or caused by external fields like e.g. gravity, are straightforward to treat. Hence all advantages of equilibrium DFT[13,14] apply to this QA or replica DFT. Also the disadvantage applies; in general the density functional is unknown. Moreover, whether one can learn anything about the important out-of-equilibrium behavior of QA systems, like hysteresis in sorption isotherms, is questionable. Based on Rosenfeld's fundamental-measure theory (FMT) for hard sphere mixtures,[15] and the subsequent discovery that one can construct density functionals by imposing the correct behavior upon dimensional reduction (i.e. in situations of extreme confinement in one or more spatial directions through

suitably chosen external potentials),[16,17] this DFT treats QA mixtures with either hard or ideal interactions.

Previous tests of QA DFT include the comparison with results from Monte Carlo (MC) simulations for the partial pair correlation functions in hard sphere systems[12] and for density profiles across the surface of a porous medium, modeled as a step-like density distribution of (freely overlapping) matrix spheres.[18] Such an interface was also investigated in a model of a random fiber network, being represented by quenched configurations of infinitely thin needle-like particles. Again comparison with simulation results shows satisfactory agreement with DFT results.[19] Much work has been devoted to a model colloid-polymer mixture where the colloids are represented as hard spheres and the polymers as freely overlapping spheres. The crucial step beyond hard sphere systems is the occurrence of a fluid-fluid phase transition, and the questions how capillary condensation occurs inside a porous medium[20] and what the structure of the interface between demixed fluid phases is like[21] were treated. A further, very promising, line of research is the application of the approach to lattice models. Note that using lattice models insight into hysteresis behavior and the relation to the appearance of a complex free energy landscape was gained.[22,23] Combining the QA-DFT approach with the very powerful lattice DFT by Lafuente and Cuesta,[24,25] freezing in a two-dimensional lattice model was investigated.[26]

In this work we consider the one-dimensional hard rod model adsorbed in a quenched matrix of rods. Two cases of interactions between the quenched particles are considered. In the first case the rods interact with a hard core potential, hence we deal with a binary QA hard rod mixture. In the second case the matrix particle are ideal (non-interacting) amongst each other, but interact with a hard-core potential with particles of the annealed component; this model is the QA analog of the model colloid-polymer mixture of Ref. 4, obtained by quenching the polymers. We use two different density functional approaches to tackle the properties of these models in both homogeneous and inhomogeneous (on average over disorder) situations. In the first approach the matrix is treated explicitly on the level of particle coordinates distributed according to the matrix Hamiltonian, and practically generated with a Monte Carlo procedure. For each matrix configuration we use Percus' functional[8] to obtain adsorbate properties, and the disorder-average over matrix configuration is carried out numerically by brute force generation of many (of the order of 1000) matrix realizations. The second approach is the QA DFT working directly on the level of the disorder-averaged adsorbate density profile, which is obtained via minimizing the disorder-averaged grand potential of the adsorbate, using the matrix density profiles as a fixed input. As the

average over disorder is taken a priori, the corresponding Euler-Lagrange equation yields directly the averaged density profile. We compare results from both theories in bulk via calculation of the partition coefficient, which is the ratio of adsorbate density inside the matrix and the density in a bulk reservoir that is in chemical equilibrium. The results from the explicit matrix averaging procedure, which we also check against an independent elementary calculation, agree well with those from the QA DFT over the full range of accessible densities. Deviations appear at high densities, which we can trace back to an incorrect behavior of the QA-DFT near close-packing. As a generic inhomogeneous situation we consider a surface of the model porous matrix, that is generated by a hard wall acting on the matrix particles (before the quench). The wall is then removed and leaves a halfspace of bulk (free of matrix particles). The adsorbate is found to exhibit density oscillations on both sides of the interface, with significantly smaller amplitude than at a hard wall.

The paper is organized as follows. In Section 2 we define the model and give an overview of its statistical mechanics and the replica trick (which can be safely skipped by an expert reader). Section 3 is devoted to both density functional methods. In Section 4 results are presented and we conclude in Sec. 5.

2. THE MODEL

2.1. Definition of the Interactions

We consider a quenched-annealed fluid mixture of a quenched species 0 with N_0 particles with one-dimensional (1d) position coordinates $x_1, x_2, \ldots x_{N_0}$ and an annealed species 1 with N_1 particles with 1d position coordinates $X_1, X_2, \ldots, X_{N_1}$. The particles interact with pairwise potentials (for pairs $\alpha\gamma = 00, 01, 11$) given by

$$\phi_{\alpha\gamma}(x) = \begin{cases} \infty & x < (\sigma_\alpha + \sigma_\gamma)/2 \\ 0 & \text{otherwise,} \end{cases} \tag{1}$$

where x is the center-center distance between two particles; σ_α is the diameter (length) of particles of species $\alpha = 0, 1$, see Fig. 1a for an illustration. This describes our first case of the hard core matrix. The total potential energy due to particle-particle interactions is $V_{00} + V_{01} + V_{11}$, with contributions

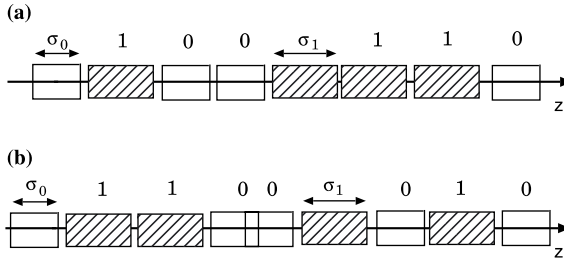$$V_{00} = \sum_{i=1}^{N_0} \sum_{j=i+1}^{N_0} \phi_{00}(|x_i - x_j|), \tag{2}$$

Fig. 1.   Model of annealed hard rods in a matrix of quenched rods in one dimension. The quenched rods interact with a) a hard core potential, and b) are ideal.

$$V_{01} = \sum_{i=1}^{N_0} \sum_{j=1}^{N_1} \phi_{01}(|x_i - X_j|), \tag{3}$$

$$V_{11} = \sum_{i=1}^{N_1} \sum_{j=i+1}^{N_1} \phi_{11}(|X_i - X_j|). \tag{4}$$

We furthermore consider the influence of external potentials, $\phi_\alpha^{\text{ext}}(x)$, acting on species $\alpha = 0, 1$, respectively. In particular $\phi_0^{\text{ext}}(x)$ acts on particles of species 0 *before* they are quenched, i.e. their density distribution is that generated in response to $\phi_0^{\text{ext}}(x)$. The resulting total external potential energy is $V_0^{\text{ext}} + V_1^{\text{ext}}$, with contributions

$$V_0^{\text{ext}} = \sum_{i=1}^{N_0} \phi_0^{\text{ext}}(x_i), \quad V_1^{\text{ext}} = \sum_{i=1}^{N_1} \phi_1^{\text{ext}}(X_i). \tag{5}$$

In our second case we consider ideal (non-interacting) matrix particles, i.e.

$$\phi_{00}(x) = 0, \tag{6}$$

valid for all distances x; the two remaining interactions are unchanged, i.e. $\phi_{01}(x)$ and $\phi_{11}(x)$ are hard core potentials given through (1); see Fig. 1b for an illustration. The size ratio $s = \sigma_1/\sigma_0$ is a geometric control parameter. In the numerical results presented below we will restrict ourselves to equally sized particles, $s = 1$, and furthermore to situations where $\phi_1^{\text{ext}}(x) = 0$.

2.2. Partition Sum, Grand Potential and Replica Trick

We first make the statistical mechanics of the quenched-annealed mixture explicit. For notational convenience the grand canonical trace

over matrix coordinates is denoted by $\int d0 \equiv \sum_{N_0=0}^{\infty} \left(N_0! \Lambda_0^{N_0} \right)^{-1} \int dx_1 \ldots$
$\int dx_{N_0}$ and that over adsorbate coordinates by $\int d1 \equiv \sum_{N_1=0}^{\infty} \left(N_1! \Lambda_1^{N_1} \right)^{-1}$
$\int dX_1 \ldots \int dX_{N_1}$, where Λ_α is the (irrelevant) thermal wavelength of species $\alpha = 0, 1$, and the position integrals run over the total system volume V. The (equilibrium) grand partition of the matrix particles under the influence of the external potential $\phi_0^{\text{ext}}(x)$ is

$$\Xi_0(\mu_0, T, V) = \int d0 e^{-\beta(V_{00} + V_0^{\text{ext}} - \mu_0 N_0)}, \tag{7}$$

where $\beta = 1/(k_B T)$, k_B is the Boltzmann constant, T is absolute temperature and μ_i is the chemical potential of species $i = 0, 1$. The grand potential for the matrix is then

$$\Omega_0(\mu_0, T, V) = -\beta^{-1} \ln \Xi_0(\mu_0, T, V). \tag{8}$$

For fixed matrix configuration $\{x_i\}$ the grand potential of the adsorbate is

$$\Omega_1(\{x_i\}, \mu_1, T, V) = -\beta^{-1} \ln \int d1 e^{-\beta(V_{11} + V_{01} + V_1^{\text{ext}} - \mu_1 N_1)}, \tag{9}$$

depending explicitly on $\{x_i\}$ through V_{01}, see (3). Note that from the viewpoint of the 1-particles, $V_{01} + V_1^{\text{ext}}$ is the *total* external potential energy. A (grand canonical) average over matrix configurations yields the disorder-averaged grand potential of the adsorbate,

$$\Omega_1(\mu_0, \mu_1, T, V)$$
$$= \Xi_0^{-1}(\mu_0, T, V) \int d0 e^{-\beta(V_{00} + V_0^{\text{ext}} - \mu_0 N_0)} \Omega_1(\{x_i\}, \mu_1, T, V). \tag{10}$$

Note that (10) has a different structure than that of the partition sum of an equilibrium mixture due to the appearance of the logarithm, upon inserting (9) into (10), *inside* the trace over the 0-particles. However, a relation to a multi-component mixture can be established using the replica trick: One introduces replicas as s copies of species 1: $\phi_{\alpha\alpha}(x) = \phi_{11}(x)$, for $1 < \alpha \leqslant s$, where s is an integer. Particles from different replicas are non-interacting, $\phi_{\alpha\gamma}(x) = 0$ for all x and $\alpha \neq \gamma$, but they interact with matrix particles in the same fashion, $\phi_{0\alpha}(x) = \phi_{01}(x)$, for $1 < \alpha \leqslant s$. Then the (equilibrium) partition sum for this $(s+1)$-component mixture can be written as

$$\Xi = \int d0 e^{-\beta(V_{00} + V_0^{\text{ext}} - \mu_0 N_0)} \left(\int d1 e^{-\beta(V_{11} + V_{01} + V_1^{\text{ext}} - \mu_1 N_1)} \right)^s, \tag{11}$$

and the grand potential is

$$\Omega(\mu_0, \mu_1, T, V; s) = -\beta^{-1} \ln \Xi. \tag{12}$$

Via analytical continuation in s, and noting that $\lim_{s \to 0} dx^s/ds = \ln x$, the disorder-averaged grand potential, (10), is obtained from the equilibrium grand potential of the replicated system as

$$\Omega_1(\mu_0, \mu_1, T, V) = \lim_{s \to 0} \frac{d}{ds} \Omega(\mu_0, \mu_1, T, V; s), \tag{13}$$

establishing a practical route to tackle the QA system via the replicated equilibrium system.

3. DENSITY FUNCTIONAL APPROACHES

The following subsections 3.1, 3.2 are valid in arbitrary space dimension d upon trivial alterations: spatial integrations become d-dimensional integrals, hence $\int dx$ is to be replaced with $\int d^d x$ and factors Λ_α are to be replaced with Λ_α^d. Although in our subsequent study we only deal with hard core interactions, where the dependence on temperature is trivial, the formalism also applies to thermal systems. Hence we consider a general binary QA mixture with arbitrary pair potentials $\phi_{\alpha\gamma}(x)$, $\alpha, \gamma = 0, 1$, not necessarily given through (1), at temperature T inside a volume V.

3.1. Equilibrium Case

In the equilibrium DFT formalism, applied to the present case, where both an explicit external potential, $\phi_1(x)$, and the (random) influence of the matrix particles at positions $\{x_i\}$ acts on the fluid, the grand potential of the adsorbate component is expressed as a functional of its one-body density distribution,

$$\tilde{\Omega}_1(\{x_i\}, [\rho_1], \mu_1, T, V) = \mathcal{F}^{id}[\rho_1] + \mathcal{F}^{exc}[\rho_1] + \int dx \rho_1(x)$$
$$\times \left[\left(\phi_1^{ext}(x) + \sum_{i=1}^{N_0} \phi_{01}(x - x_i) \right) - \mu_1 \right], \tag{14}$$

where $\mathcal{F}^{id}[\rho_1] = \beta^{-1} \int dx \rho_1(x)[\ln(\rho_1(x)\Lambda_1) - 1]$ is the (Helmholtz) free energy functional of the ideal gas, $\mathcal{F}^{exc}[\rho_1]$ is the excess (over ideal) contribution that arises from interactions between (adsorbate) particles, and the

term in round brackets is the *total* external potential acting on the adsorbate stemming from the explicit (non-random) external potential, $\phi_1^{\text{ext}}(x)$, and the sum over interactions with (randomly distributed) matrix particles. The latter contribution is parameterized by the set of matrix coordinates $\{x_i\}$, and hence $\tilde{\Omega}_1$ depends explicitly on $\{x_i\}$, which we stress in the notation of the l.h.s. of (14). The free energy functionals $\mathcal{F}^{\text{id}}$ and $\mathcal{F}^{\text{exc}}$ depend on T and V; this is suppressed in the notation in (14) and in the following. The minimization condition is

$$\left. \frac{\delta\tilde{\Omega}(\{x_i\}, [\rho_1], \mu_1, T, V)}{\delta\rho_1} \right|_{\rho_1 = \rho_1(\{x_i\}, x)} = 0, \tag{15}$$

where $\rho_1(\{x_i\}, x)$ is the adsorbate density distribution that solves (15). The value of the grand potential is then obtained by reinserting the solution into the grand potential functional,

$$\Omega(\{x_i\}, \mu_1, T, V) = \tilde{\Omega}(\{x_i\}, [\rho_1(x, \{x_i\})], \mu_1, T, V), \tag{16}$$

from which the average over the disorder, $\Omega(\mu_0, \mu_1, T, V)$, can be obtained via (10). In a similar way as for the grand potential, the matrix-averaged adsorbate density profile is given as

$$\rho_1(x) = \Xi_0^{-1}(\mu_0, T, V) \int d0 e^{-\beta(V_{00}+V_0^{\text{ext}}-\mu_0 N_0)} \rho_1(x, \{x_i\}). \tag{17}$$

Note that *explicit* averages over the matrix configurations are to be performed in (10) and (17). In the numerical procedure described below, we will carry this out numerically via a Monte Carlo procedure.

3.2. Quenched-Annealed Case

Here we first formulate the equilibrium DFT of the replicated model from which we obtain, in the appropriate limit of vanishing number of components, the minimization condition of DFT for one quenched and one annealed component. Explicitly assuming absence of replica symmetry breaking, hence $\rho_1(x) = \rho_\alpha(x)$, $1 < \alpha \leqslant s$, the grand potential functional for the replicated *equilibrium* mixture reduces to

$$\tilde{\Omega}([\rho_0, \rho_1], \mu_0, \mu_1, T, V; s) \equiv \tilde{\Omega}([\{\rho_\alpha\}], \{\mu_\alpha\}, T, V) \tag{18}$$

The minimization conditions are

$$\frac{\delta \tilde{\Omega}([\rho_0, \rho_1], \mu_0, \mu_1, T, V; s)}{\delta \rho_\alpha(x)} = 0, \quad \alpha = 0, 1, \tag{19}$$

which are two *coupled* equations for the two unknown functions $\rho_0(x)$ and $\rho_1(x)$. At the minimum the value of the functional is the true grand potential

$$\Omega(\mu_0, \mu_1, V, T; s) = \tilde{\Omega}([\rho_0, \rho_1], \mu_0, \mu_1, T, V; s). \tag{20}$$

Via analytic continuation, and Taylor expanding in s around $s = 0$, one obtains

$$\tilde{\Omega}([\rho_0, \rho_1], \mu_0, \mu_1, T, V; s) = \tilde{\Omega}_0([\rho_0], \mu_0, T, V)$$
$$+ s\tilde{\Omega}_1([\rho_0, \rho_1], \mu_1, T, V) + O(s^2), \tag{21}$$

where $\tilde{\Omega}_0$ is the grand potential of the pure system of 0-particles, that may formally be written as $\tilde{\Omega}_0([\rho_0], \mu_0, T, V) = \tilde{\Omega}([\rho_0, 0], \mu_0, \mu_1 \to -\infty, T, V)$, furthermore $\tilde{\Omega}_1[\rho_0, \rho_1] = \lim_{s \to 0} d\tilde{\Omega}([\rho_0, \rho_1], \mu_0, \mu_1, T, V; s)/ds$. Note that via this definition $\tilde{\Omega}_1$ is also the disorder-averaged grand potential, given in (13).

We decompose both contributions in the standard way:

$$\tilde{\Omega}_0([\rho_0], \mu_0, T, V) = \mathcal{F}^{\text{id}}[\rho_0] + \mathcal{F}_0^{\text{exc}}[\rho_0] + \int dx \rho_0(x) \left(\phi_0^{\text{ext}}(x) - \mu_0\right), \tag{22}$$

$$\tilde{\Omega}_1([\rho_0, \rho_1], \mu_1, T, V) = \mathcal{F}^{\text{id}}[\rho_1] + \mathcal{F}_1^{\text{exc}}[\rho_0, \rho_1] + \int dx \rho_1(x) \left(\phi_1^{\text{ext}}(x) - \mu_1\right), \tag{23}$$

which can be viewed as definitions for the excess (over ideal gas) free energy functionals, $\mathcal{F}_0^{\text{exc}}[\rho_0]$ and $\mathcal{F}_1^{\text{exc}}[\rho_0, \rho_1]$, that arise from interactions between particles. Note, however, that neither $\mathcal{F}^{\text{id}}[\rho_0]$ nor a contribution involving $\phi_0^{\text{ext}}(x)$ appear on the r.h.s. of (23), in contrast to the binary equilibrium case.

We insert the small-s-expansion of the grand potential functional, (21), into the equilibrium minimization condition, (19). Performing the limit $s \to 0$, the minimization conditions for the QA mixture result as

$$\frac{\delta \tilde{\Omega}_0([\rho_0], \mu_0, T, V)}{\delta \rho_0(x)} = 0, \tag{24}$$

$$\frac{\delta \tilde{\Omega}_1([\rho_0, \rho_1], \mu_1, T, V)}{\delta \rho_1(x)} = 0. \tag{25}$$

The derivation of (24) is straightforward. To obtain (25) one sets $\alpha = 1$ in (19) i.e. differentiates w.r.t. to $\rho_1(x)$ and divides the resulting equation by s, assuming $s > 0$, before taking the limit $s \to 0$. Note that (24) is decoupled from (25), hence in particular $\rho_0(x)$ is solely determined through (24). The result then serves as an input to (25), which is solely to be solved for $\rho_1(x)$.

3.3. Excess Free Energy Functionals

The theoretical approaches described so far incorporate the complexity of the problem i) in the excess free energy functionals for the adsorbate, $\mathcal{F}^{\mathrm{exc}}[\rho_1]$, and an explicit average over matrix configurations, and ii) in excess free energy functionals for the matrix component, $\mathcal{F}_0^{\mathrm{exc}}[\rho_0]$, and for the adsorbate in the presence of the matrix, $\mathcal{F}_1^{\mathrm{exc}}[\rho_0, \rho_1]$. For the present 1d model, the situations is fortunate, as an exact result for $\mathcal{F}^{\mathrm{exc}}[\rho_1]$ and $\mathcal{F}_0^{\mathrm{exc}}[\rho_0]$ is available, namely Percus' free energy functional for 1d hard rods.[8,9] For a one-component system of hard rods of species α one writes (using Rosenfeld's terminology)

$$\mathcal{F}^{\mathrm{exc}}[\rho_\alpha] = \int dx\, n_\alpha^{(0)}(x) \Phi_{\mathrm{hc}}'\left(n_\alpha^{(1)}(x)\right), \tag{26}$$

where the weighted densities, $n_\alpha^{(0)}(x)$ and $n_\alpha^{(1)}(x)$, are obtained from the bare density profile (of species α) via

$$n_\alpha^{(0)}(x) = [\rho_\alpha(x - R_\alpha) + \rho_\alpha(x + R_\alpha)]/2, \tag{27}$$

$$n_\alpha^{(1)}(x) = \int_{x - R_\alpha}^{x + R_\alpha} dx'\, \rho_\alpha(x'), \tag{28}$$

where $R_\alpha = \sigma_\alpha/2$ is the particle "radius" of species $\alpha = 0, 1$, and the upper index $\nu = 0, 1$ of the weighted density is related to its dimension, which is (length)$^{\nu - d}$, where $d = 1$ is the space dimension. The prime in (26) denotes differentiation w.r.t. the argument, and $\Phi_{\mathrm{hc}}(\eta)$ is the zero-dimensional free energy of hard core particles,[16] given by

$$\Phi_{\mathrm{hc}}(\eta) = (1 - \eta)\ln(1 - \eta) + \eta. \tag{29}$$

Our (approximate) QA functional has very similar structure.[12] We start from the generalization of (26) to binary mixtures, which is

$$\mathcal{F}_1^{\mathrm{exc}}[\rho_0, \rho_1] = \int dx \sum_{\alpha = 0,1} n_\alpha^{(0)}(x) \Phi_\alpha\left(n_0^{(1)}(x), n_1^{(1)}(x)\right), \tag{30}$$

where the weighted densities are still given through (27) and (28), and derivatives of the zero-dimensional free energy, Φ, are defined as $\Phi_\alpha(\eta_0, \eta_1) = \partial\Phi(\eta_0, \eta_1)/\partial\eta_\alpha$. The particular form (30) ensures that the exact result for Φ is recovered if the functional is applied to a zero-dimensional density distribution, defined as $\rho_i(x) = \eta_i\delta(x)$ for $i = 0, 1$. Hence it can be shown via elementary calculation that $\Phi(\eta_0, \eta_1) = \mathcal{F}_1^{\text{exc}}[\eta_0\delta(x), \eta_1\delta(x)]$. The exact result for $\Phi(\eta_0, \eta_1)$ is obtained by solving the zero-dimensional limit (where all particles present in the system overlap); a detailed calculation can be found in Ref. 12. Such a situation can be enforced by appropriate external potentials $\phi_\alpha^{\text{ext}}(x) = \infty$ if $|x| > L$ and zero otherwise, and represents a "cavity" of size L, where $L \ll \min(\sigma_0, \sigma_1)/2$. Hence any two particles (of species α and γ) present in the system will overlap, i.e. $x < \sigma_{\alpha\gamma}$, where x is the center-center distance between both particles. (As a consequence the density profiles vanish outside the cavity, $\rho_\alpha(|x| > L/2) = 0$.) This constitutes the crucial simplification that allows to calculate the free energy; its excess contribution is independent of L.[12] In the case of the hard core matrix the result is

$$\Phi(\eta_0, \eta_1) = (1 - \eta_0 - \eta_1)\ln(1 - \eta_0 - \eta_1) + \eta_1 - (1 - \eta_0)\ln(1 - \eta_0).$$
(31)

It is interesting to note that in this special case there is a simple relation to the corresponding fully annealed binary hard core mixture: $\Phi(\eta_0, \eta_1) = \Phi_{\text{hc}}(\eta_0 + \eta_1) - \Phi_{\text{hc}}(\eta_0)$. In the case of the ideal matrix the result for the excess free energy is

$$\Phi(\eta_0, \eta_1) = \left(e^{-\eta_0} - \eta_1\right)\ln\left(e^{-\eta_0} - \eta_1\right) + \eta_1 + \eta_0 e^{-\eta_0}.$$
(32)

This does not have a similar relation as above to the corresponding fully annealed binary mixture (the colloid-polymer mixture of Ref. 4). As a further aside, we note that setting $\Phi(\eta_0, \eta_1) = \Phi_{\text{hc}}(\eta_0 + \eta_1)$ in (30) gives the exact excess free energy functional for equilibrium (where both species are annealed) binary hard rods.[8,9]

The density functional thus defined is exact on the second virial level, which can be seen by Taylor expanding $\Phi(\eta_0, \eta_1)$ in both arguments to second order, and exploiting the property of the weight functions to recover the Mayer bond upon convolution.

3.4. Numerical Procedure

In order to calculate density profiles, the minimization is done with a standard iteration technique. We chose a very fine grid with spacing

0.0002σ to discretize the space coordinate. The system is assumed to be periodic in x with length 20σ. To generate the matrix configurations $\{x_i\}$, a Monte Carlo scheme is used. We start from an initial configuration where the (matrix) particles have equally-spaced positions. Then particle displacements are performed according to the Metropolis algorithm, i.e. a new position is only accepted if no overlap with any other (matrix) particle or with the wall (introduced below) occurs. 1000 MC moves per particle are performed for equilibration, and 100 MC moves per particle are performed between configurations that are used for data production. For given matrix configuration $\{x_i\}$ the density profile for the adsorbate component, $\rho_1(x, \{x_i\})$, is then obtained from solution of the minimization condition of the equilibrium DFT, (15). Results from 1000 independent matrix realizations for each N_0 in the range $N_1 = 0 - 20$ are then used to carry out the average over the disorder and obtain $\rho_1(x)$ via (17).

4. RESULTS

4.1. Bulk

The bulk case constitutes the basis of the subsequent interface study, and is considered for the following three reasons: i) to assess the accuracy of the QA-DFT, ii) to demonstrate the correctness of the matrix-averaging procedure via comparing with an independent elementary calculation, and iii) to study the (exact) partition coefficient, which we find to possess (very unusual) non-monotonic behavior.

The matrix particles are distributed homogeneously on average, and hence are characterized by a one-body density distribution $\rho_0(x) = \eta_0/\sigma_0 =$ const. As a consequence, the adsorbate density distribution is on average $\rho_1(x) = \eta_1/\sigma_1 =$ const. We imagine the system to be in chemical equilibrium with a reservoir of hard rods of species 1 of packing fraction $\eta_1^r = \rho_1^r \sigma_1$, where ρ_1^r is the number density in the reservoir; there are no quenched matrix particles in the reservoir. The reservoir density sets the chemical potential of 1-particles via the (well-known) hard rod equation of state,

$$\beta\mu_1 = \ln(\eta_1^r \Lambda_1/\sigma_1) - \ln(1 - \eta_1^r) + \frac{\eta_1^r}{1 - \eta_1^r}. \tag{33}$$

The central quantity that we use to characterize the coupled systems is the partition coefficient $K = \eta_1/\eta_1^r = \rho_1/\rho_1^r$, which we will study as a function of the reservoir packing fraction η_1^r.

Before applying both DFT methods to this case, we first seek to obtain a benchmark result for $K(\eta_1^r)$ from an independent, elementary calculation; see ref. 27 for more mathematical background and ref. 7 for an alternative application. We start from the probability $W(x)dx$ that the nearest-neighbor distance for 0-particles (measured between their centers) is between x and $x + dx$ (we call this a gap of size x), given by

$$W(x)\sigma_0 = \begin{cases} \frac{\eta_0}{1-\eta_0} \exp\left(\frac{\eta_0}{1-\eta_0}(1-x/\sigma_0)\right) & x > \sigma_0 \\ 0 & \text{otherwise,} \end{cases} \tag{34}$$

from which the average nearest-neighbor distance between matrix particles follows as $\bar{x} = \int dx\, x\, W(x) = \sigma_0/\eta_0$, which is an expected result. To derive (34), note that the occurrence of a gap of size x is proportional to the Boltzmann weight of the reversible mechanical work to create it, hence $W(x) \propto \exp(-P_0 x)$, where P_0 is the pressure of the bulk (matrix) system, given for one-dimensional hard rods by $\sigma_0 \beta P_0 = \eta_0/(1-\eta_0)$. One obtains the precise form of (34) by taking into account the correct normalization, $\int_0^\infty dx\, W(x) = 1$.

The average number of 1-particles in a gap of (fixed) size x between two 0-particles is $\bar{N}_1(x, \mu_1) = \beta^{-1}\partial \ln \Xi_1/\partial \mu_1$, where the partition sum of 1-particles in the gap of volume $x - \sigma_0 - \sigma_1$ (being accessible to the centers of 1-particles) is

$$\begin{aligned} \Xi_1(x, \mu_1) &= \int d1 \exp(-\beta(V_{11} - \mu_1 N_1)) \\ &= \sum_{N_1=0}^{\infty} \frac{\exp(\beta\mu_1 N_1)}{\Lambda_1^{N_1} N_1!} (x - \sigma_0 - N_1\sigma_1)^{N_1}. \end{aligned} \tag{35}$$

The mean number of 1-particles in the gap between two neighboring 0-particles, averaged over all sizes of the gap, is $\bar{N}_1(\mu_1) = \int dx\, W(x)\bar{N}_1(x, \mu_1)$. Then the average density of 1-particles is $\rho_1 = \bar{N}_1(\mu_1)/\bar{x} = \bar{N}_1(\mu_1)\eta_0/\sigma_0$, from which the partition coefficient results as $K = \rho_1/\rho_1^r = \bar{N}_1\sigma_1/(\bar{x}\eta_1^r)$. Putting things together,

$$K = \frac{\eta_0 \sigma_1}{\eta_1^r \sigma_0} \int_0^\infty dx\, W(x) \frac{\partial \ln \Xi_1(x, \mu_1)}{\partial \beta \mu_1}, \tag{36}$$

where the equation of state in the reservoir of 1-particles, (33), can be used to obtain μ_1 in terms of η_1^r in (36), hence K is solely a function of the packing fractions η_0, η_1^r and of the size ratio σ_1/σ_0. In general, we solve

(36) numerically; we can, however, obtain analytic results in both (extreme) cases of high and low reservoir density,

$$K(\eta_1^r \to 0) = (1 - \eta_0) \exp(-s\eta_0/(1 - \eta_0)), \tag{37}$$

$$K(\eta_1^r \to 1) = \frac{s\eta_0}{\exp(s\eta_0/(1 - \eta_0)) - 1}, \tag{38}$$

where $s = \sigma_1/\sigma_0$. (38) is obtained by noting that for $\mu_1 \to \infty$ the mean number of 1-particles equals the maximal possible number, i.e. $\bar{N}_1(x, \mu_1 \to \infty) = \mathrm{floor}((x - \sigma_0)/\sigma_1)$, where $\mathrm{floor}(x)$ gives the next integer smaller than x.

In the case of the of the non-interacting matrix, the equation of state of the 0-particles is that of an ideal gas, $\sigma_0 \beta P = \eta_0$. The gap size distribution is

$$W(x) = (\eta_0/\sigma_0) \exp(-\eta_0 x/\sigma_0), \quad x > 0, \tag{39}$$

from which K can be derived following the same steps as above. Again in the two limiting cases of either high or low reservoir packing fraction analytic expression can be obtained for the partition coefficient,

$$K(\eta_1^r \to 0) = \exp(-(1 + s)\eta_0), \tag{40}$$

$$K(\eta_1^r \to 1) = \frac{s\eta_0 \exp(-\eta_0)}{\exp(s\eta_0) - 1}. \tag{41}$$

In order to obtain K from the QA DFT, we use the predicted equation of state, which is in the case of the hard core matrix

$$\beta\mu_1 = \ln(\eta_1 \Lambda_1/\sigma_1) - \ln(1 - \eta_0 - \eta_1) + \frac{\eta_1 + s\eta_0}{1 - \eta_0 - \eta_1}, \tag{42}$$

which we set equal to the chemical potential in the reservoir, (33). For small η_1^r this gives the exact result, (37). In the high density limit, however, we do not recover (38), but obtain $K(\eta_1^r \to 1) = 1 - \eta_0$. Note that the small η_0-expansion of the exact result, (38), is $K(\eta_1 = 1) = 1 - (1 + s/2)\eta_0 + O(\eta_0^2)$, differing already in linear oder. For intermediate values of η_1^r we obtain numerical solutions.

Results for K as a function of reservoir packing fraction, η_1^r, are displayed in Fig. 2a for three different matrix packing fractions, $\eta_0 = 0.1, 0.5, 0.7$. For the lowest value considered, $\eta_0 = 0.1$, K slightly increases as a function of η_1^r. Remarkably a maximum is reached at $\eta_1^r \sim$
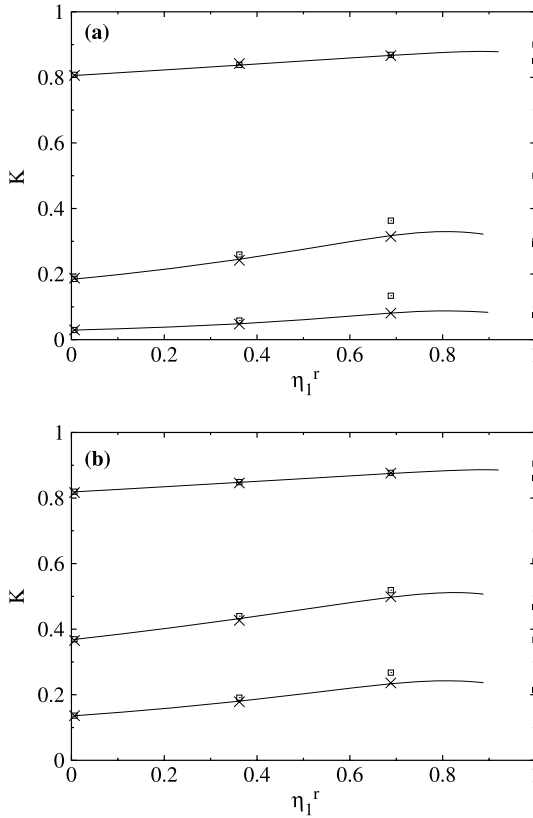
Fig. 2. Partition coefficient $K = \eta_1/\eta_1^r$ for 1d hard rods immersed in a 1d matrix of quenched rods as a function of the packing fraction in a reservoir of rods, η_1^r. Shown are results from the elementary calculation, (36), (lines and full squares), DFT with explicit matrix averaging (crosses) and QA DFT (open squares). a) Matrix particles are interacting with a hard core potential and possess packing fraction $\eta_0 = 0.1, 0.5, 0.7$ (from top to bottom). b) Matrix particles are ideal and posses packing fraction $\eta_0 = 0.1, 0.5, 1$ (from top to bottom).

0.9, significantly smaller than the close-packing limit, $\eta_1^r = 1$. We could not obtain numerical results for $0.9 < \eta_1^r < 1$, but the available data clearly tend towards the limiting value, obtained through (38). For the intermediate value $\eta_0 = 0.5$ the variation of K with η_1^r is stronger and the maximum is more pronounced. For $\eta_1^r = 0.7$ hardly any adsorbate particles can enter the matrix and the resulting values are $K \lesssim 0.1$, the variation with η_1^r being similar to the above cases. The exact results plotted in Fig. 2 are obtained from the elementary calculation above (lines) and from the

DFT with explicit matrix averaging described in Sec. 3.1. Both agree with high numerical accuracy. The result from the QA DFT is exact in the low-density limit and stays accurate for intermediate η_1^r. At $\eta_1^r \sim 0.7$ deviations emerge, overestimating the values of K. Moreover, the maximum is absent, and monotonic increase with η_1^r is found. We hence conclude that the overall performance of the QA DFT is very satisfactory, but that the intriguing non-monotonic behavior near close-packing is missed.

The situation in the case of the ideal matrix is similar. The equation of state from QA DFT is

$$\beta\mu_1 = \ln(\eta_1\Lambda_1/\sigma_1) - \ln\left(e^{-\eta_0} - \eta_1\right) + \frac{s\eta_0 e^{-\eta_0} + \eta_1}{e^{-\eta_0} - \eta_1}. \tag{43}$$

Again the result from QA DFT for $\eta_1^r \to 0$ equals the exact result, (41). In the limit $\eta_1^r \to 1$ the result from QA DFT is $K(\eta_1^r \to 1) = \exp(-\eta_0)$, which overestimates the exact expression, (41). See Fig. 2b) for numerical results for K as a function of η_1^r for matrix packing fractions $\eta_0 = 0.1, 0.5, 1$. Compared to the case of the hard core matrix, at equal densities K is larger, clearly due to the more open void structure of the ideal matrix particles. Again K displays a maximum near $\eta_1^r \sim 0.8$, which is not captured within the QA DFT. Nevertheless, the overall agreement is again very reasonable, and gives us confidence to turn to inhomogeneous situations.

4.2. Behavior at the Matrix Surface

We consider matrix distributions that are generated by a hard wall, described by the external potential

$$\phi_0^{\text{ext}}(x) = \begin{cases} 0 & x > 0 \\ \infty & \text{otherwise}, \end{cases} \tag{44}$$

acting before the quench. In order to obtain $\rho_0(x)$, we solve the minimization condition, (24), using Percus' functional, given through (26)–(29), as $\mathcal{F}_0^{\text{exc}}$ in (22). This provides an exact (numerical) solution, see (Fig. 3a) for matrix density profiles for three different matrix packing fractions $\eta_0 = 0.1, 0.5, 0.7$. As η_0 increases the contact value at the wall increases and the layering near the wall becomes more pronounced, i.e. the amplitude of the density oscillations grows.

The density profile of the adsorbate being exposed to such an inhomogeneous matrix (note that the hard wall, (44), only acts on the matrix particles) are obtained using either the explicit matrix-averaging procedure
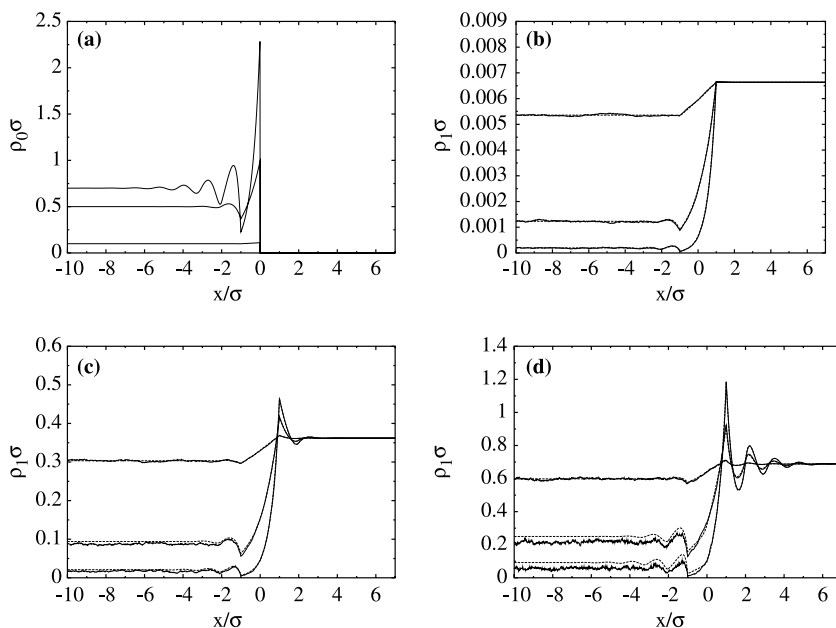
Fig. 3. Behavior of adsorbate particles near the surface of a matrix of quenched rods immersed in a hard core matrix. a) Density profile of the matrix particles, $\sigma \rho_0(x)$, as a function of the scaled distance x/σ for packing fractions $\eta_0 = 0.1, 0.5, 0.7$ (from bottom to top). Adsorbate density profiles $\sigma \rho_1(x)$ are shown for η_0 (from top to bottom) for $\beta \mu_1 = -5$ (b), 0 (c), and 3 (d). Results from the QA DFT (dashed lines) are compared with those of the exact treatment (full lines).

of Sec. 3.1 or the QA DFT of Sec. 3.2. In Fig. 3b-d we display results for $\rho_1(x)$ for $\eta_0 = 0.1, 0.5, 0.7$. For $x > 0$ far away from the surface, the reservoir value is reached, $\rho_1(x \to \infty) = \rho_1^r$; for $x < 0$ deep inside the matrix, the asymptotic value is $\rho_1(x \to -\infty) = K\rho_1^r$, as studied above. For the lowest adsorbate density considered, result for $\beta \mu_1 = -5$ are displayed in Fig. 3, the crossover between the limiting cases happens in a narrow interval $-\sigma < x < \sigma$. Already for $x > \sigma$ the profile is flat. Inside the matrix, however, for $x < \sigma$ there are small oscillations with wavelength of the order of σ that decay rapidly with increasing distance from the surface. These oscillations are not due to the correlations between adsorbate particles, but are merely "imprinted" by the inhomogeneous *matrix* profiles as shown in Fig. 3a. Increasing the adsorbate chemical potential, see Fig. 3c for $\beta \mu_1 = 0$, leads to stronger structuring outside the matrix, $x > \sigma$. This layering is similar to that at a hard wall, but with significantly smaller amplitude. Clearly, this "washing out" is due to the average over the disorder. Note that for a given matrix configuration $\{x_i\}$ the matrix particle closest

to the surface, say x_{N_0}, exerts a hard interaction on the fluid particles with $X_j > x_{N_0}$, and indeed the resulting $\rho_1(x)$ is that of a hard wall. The disorder-average then leads to the "washing out". For $\beta\mu_1 = 3$, shown in Fig. 3d, even stronger layering is observed. As expected from the bulk analysis above, the QA DFT overestimates K and hence the adsorbate density inside the matrix, which is clearly visible for $x < -\sigma$. The shape of the curves, however, is predicted very accurately. Moreover, for $x > -\sigma$, the QA DFT lies practically on top of the exact result.

In the case of the ideal matrix particles exposed to the hard wall, Eq. 44, leads to step function density profiles, see Fig. 4a, hence is very different from highly structured profile of the hard core matrix, Fig. 3. The general trends upon varying the matrix density and the adsorbate chemical potential, see Fig. 4b-d for results for the same values of $\beta\mu_1$ as above, is similar. The ideal matrix allows to consider higher matrix packing fractions, and we have gone up to $\eta_0 = 1$. It is to be noted that oscillations do appear for $x < \sigma$, although the matrix profile is uniform. These oscillations clearly arise from packing effects between adsorbate particles. Again the results from the QA DFT agree very well with those of the exact calculation.
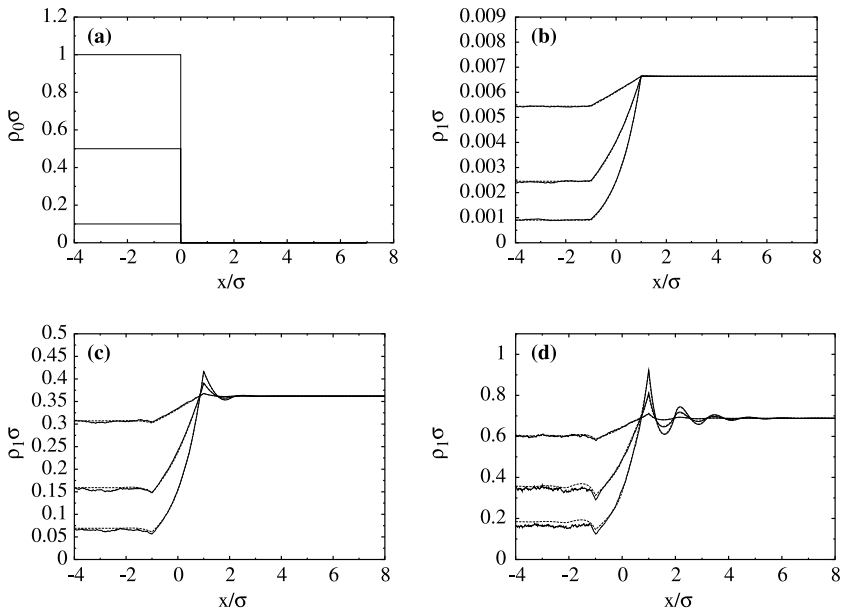

Fig. 4. Same as Fig. 3, but for ideal matrix particles of packing fraction $\eta_0 = 0.1, 0.5, 1$.

5. CONCLUSIONS

In conclusion we have applied a recent DFT for adsorbate fluids in random matrices to the one-dimensional hard core model. Comparing with analytic and numerical exact solutions in bulk and at matrix interfaces we have tested the accuracy of the QA DFT. The general performance is remarkable, both for the bulk partition coefficient and for the inhomogeneous density profiles. Subtleties like non-monotonic variation of the partition coefficient upon increasing adsorbate density are not captured by the QA DFT.

We note that by confining mesoscopic colloidal particles in narrow channels[28] one-dimensional model fluids are experimentally accessible. In principle we could imagine modifying setups of confining groves as described in ref. 28 in order to prepare model systems that resemble the model described in the current work. Possible future work could be devoted to the impact of quenched disorder on three-dimensional narrow channels.[29,30] Furthermore, it would be interesting to study the asymptotic decay of correlation functions[31,32] of fluids with quenched disorder more systematically. Finally, whether non-monotonic variation of the partition coefficient appears in 3d hard core models is an intriguing question.

6. ACKNOWLEDGMENTS

REFERENCES

1. L. Tonks, *Phys. Rev.* **50**:955 (1936).
2. H. N. W. Lekkerkerker and B. Widom, *Physica A* **285**:483 (2000).
3. S. M. Oversteegen and H. N. W. Lekkerkerker, *Physica A* **310**:181 (2002).
4. J. M. Brader and R. Evans, *Physica A* **306**:287 (2002).
5. U. Marini Bettolo Marconi, and P. Tarazona, *J. Chem. Phys.* **110**:8032 (1999).
6. F. Penna and P. Tarazona, *J. Chem. Phys.* **119**:1766 (2003).
7. R. D. Kaminsky and P. A. Monson, *Langmuir* **9**:561 (1993).
8. J. K. Percus, *J. Stat. Phys.* **15**:505 (1976).
9. J. K. Percus, *J. Stat. Phys.* **28**:67 (1982).
10. W. G. Madden and E. D. Glandt, *J. Stat. Phys.* **51**:537 (1988).
11. J. A. Given and G. Stell, *J. Chem. Phys.* **97**:4573 (1992).

12. M. Schmidt, *Phys. Rev. E* **66**:041108 (2002).
13. R. Evans, *Adv. Phys.* **28**:143 (1979).
14. R. Evans, in *Fundamentals of Inhomogeneous Fluids*, D. Henderson, ed. (Dekker, New York, 1992), Chap. 3, p. 85.
15. Y. Rosenfeld, *Phys. Rev. Lett.* **63**:980 (1989).
16. Y. Rosenfeld, M. Schmidt, H. Löwen, and P. Tarazona, *Phys. Rev. E* **55**:4245 (1997).
17. P. Tarazona and Y. Rosenfeld, *Phys. Rev. E* **55**, R4873 (1997).
18. M. Schmidt, *Phys. Rev. E* **68**:021106 (2003).
19. M. Schmidt and J. M. Brader, *J. Chem. Phys.* **119**:3495 (2003).
20. M. Schmidt, E. Schöll-Paschinger, J. Köfinger, and G. Kahl, *J. Phys. Condens. Matter* **14**:12099 (2002).
21. P. P. F. Wessels, M. Schmidt, and H. Löwen, *Phys. Rev. E* **68**:061404 (2003).
22. E. Kierlik, P. A. Monson, M. L. Rosinberg, L. Sarkisov, and G. Tarjus, *Phys. Rev. Lett.* **87**:055701 (2001).
23. E. Kierlik, P. A. Monson, M. L. Rosinberg, and G. Tarjus, *J. Phys. Condens. Matter* **14**:9295 (2002).
24. L. Lafuente and J. A. Cuesta, *Phys. Rev. Lett.* **89**:145701 (2002).
25. L. Lafuente and J. A. Cuesta, *J. Phys. Condens. Matter* **14**:12079 (2002).
26. M. Schmidt, L. Lafuente, and J. A. Cuesta, *J. Phys. Condens. Matter* **15**:4695 (2003).
27. S. Torquato, B. Lu, and J. Rubinstein, *Phys. Rev. A* **41**:2059 (1990).
28. Q. -H. Wei, C. Bechinger, and P. Leiderer, *Science* **287**:625 (2000).
29. D. Goulding, J. P. Hansen, and S. Melchionna, *Phys. Rev. Lett.* **85**:1132 (2000).
30. D. Goulding, S. Melchionna, and J. P. Hansen, *Phys. Chem. Chem. Phys.* **3**:1644 (2001).
31. R. Evans, J. R. Henderson, D. C. Hoyle, A. O. Parry, and Z. A. Sabeur, *Mol. Phys.* **80**:755 (1993).
32. R. Evans, R. J. F. Leote de Carvalho, J. R. Henderson, and D. C. Hoyle, *J. Chem. Phys.* **100**:591 (1994).